Pharmacology, Biochemistry and Behavior 92 (2009) 635–641

Contents lists available at ScienceDirect

Pharmacology, Biochemistry and Behavior

journal homepage: www.elsevier.com/locate/pharmbiochembeh

# Protective effect of Z-ligustilide against amyloid β-induced neurotoxicity is associated with decreased pro-inflammatory markers in rat brains

Xi Kuang, Jun-Rong Du *, Ya-Shu Chen, Jing Wang, Yan-Nan Wang

*State Key Laboratory of Biotherapy, West China Medical School, Sichuan University, Chengdu, 610041, China*
*Department of Pharmacology and Biopharmaceutics, West China School of Pharmacy, Sichuan University, Chengdu, 610041, China*
*Key Laboratory of Drug Targeting, Education Ministry, West China School of Pharmacy, Sichuan University, Chengdu, 610041, China*

ARTICLE INFO

*Article history:*
Received 5 September 2008
Received in revised form 20 February 2009
Accepted 11 March 2009
Available online 24 March 2009

*Keywords:*
Alzheimer's disease (AD),
Z-ligustilide (LIG),
Amyloid $\beta_{25-35}$,
Neuroinflammatory response
Morris water maze

ABSTRACT

Neuroinflammatory responses induced by accumulation and aggregation of β-amyloid (Aβ) peptide are mainly involved in Alzheimer's disease (AD) pathogenesis. Z-ligustilide (LIG), a novel neuroprotectant against ischemic stroke, was reported to have significant anti-inflammatory effects via inhibition of TNF-α production and bioactivity. The present study investigated the effect of LIG on AD-like cognitive impairment and neuropathological and neuroinflammatory changes induced by bilateral intracerebroventricular injections of $A\beta_{25-35}$ at a dose of 50 nmol/rat. Rats received oral administration of 40 mg/kg LIG or volume-matched vehicle 1 h before $A\beta_{25-35}$ treatment then once daily for 15 days. Morris water maze was used to detect the cognitive dysfunction induced by $A\beta_{25-35}$. Compared to the sham-operated rats, $A\beta_{25-35}$ injection significantly prolonged the mean escape latency in vehicle-treated rats in the Morris water maze test ($p<0.01$) and increased both AD-related neuropathological signs (i.e., Aβ, amyloid precursor protein, and phosphorylated Tau immunoreactivity) and pro-inflammatory mediators (i.e., TNF-α and activated NF-κB) in the prefrontal cortex and CA1 subregion of the hippocampus. And these neurotoxic effects of $A\beta_{25-35}$ were significantly ameliorated with LIG treatment ($p<0.01$ *vs.* vehicle-treated group). The present data suggest that LIG modulates TNF-α-activated NF-κB signaling pathway with respect to its protective effect against $A\beta_{25-35}$-induced neurotoxicity. LIG would be a potential candidate for further preclinical study aimed at the prevention and treatment of cognitive deficits in AD.



## 1. Introduction

Alzheimer's disease (AD) is a progressive neurodegenerative disorder which is characterized by damage of the brain regions associated with learning and memory (Bussière et al., 2003; Gomez-Isla et al., 1996; West et al., 1994). A remarkable rise in life expectancy during the past century has made AD the most common form of neurodegenerative disorder and the fourth leading cause of death in developed nations. Current therapeutic strategies, such as cholinesterase inhibitor preservation of cholinergic neuron neurotransmitters (Husain et al., 2008), have failed to provide an effective cure or prevention for AD. However, epidemiologic studies suggest that prophylactic treatment with anti-inflammatory agents decrease the risk of developing AD (McGeer and McGeer, 2001; Pasinetti, 2002). Neuroinflammation is well established to be involved in AD pathogenesis (Akiyama et al., 2000; Eikelenboom et al., 2008). Reactive astrogliosis and microgliosis are often found in areas of amyloid β (Aβ) plaque deposits in AD brains (Bales et al., 2000). Activated glial cells initiate a sequence of molecular and cellular events that involve the activation of nuclear factor-κB (NF-κB), a transcription factor that is responsible for the expression of multiple genes involved in physiological processes and inflammatory responses (Akama et al., 1998; Bales et al., 1998) and the formation of reactive oxygen species (ROS) that lead to cellular damage in AD (Colton et al., 2000). Aβ consisting of 39 to 42 amino acid residues is proteolytically produced by β- and γ-secretases from a single transmembrane amyloid precursor protein (APP). Experimental and genetic evidence has demonstrated that the accumulation and aggregation of Aβ in brain plays a causal role in initiating the inflammatory and neurotoxic cascades that occur in AD (Selkoe et al., 1986; Whitehead et al., 2005).

Z-ligustilide (3-butylidene-4,5-dihydrophthalide, LIG) has been considered to be the main active ingredient of many *Umbelliferae* medicinal plants (Lin et al., 1979; Naito et al., 1996). LIG was reported to have an anti-inflammatory effect by inhibiting TNF-α production and TNF-α-induced NF-κB activation *in vitro* (Liu et al., 2005). Our recent studies demonstrated that LIG exerted significant neuroprotection against cerebral ischemic damage in various *in vivo* and *in vitro* stroke models (Kuang et al., 2006; Kuang et al., 2008; Peng et al., 2007; Yu et al., 2008). On the basis of these previous studies, we hypothesized that LIG might also exert neuroprotection against AD through an anti-inflammatory process. In addition, most AD patients show gradual impairment of cognitive capabilities, which is associated

* Corresponding author. Tel./fax: +86 28 85503938.
*E-mail address:* dujr07@gmail.com (J.-R. Du).

0091-3057/$ – see front matter © 2009 Elsevier Inc. All rights reserved.
doi:10.1016/j.pbb.2009.03.007

with hippocampus and the prefrontal cortex (PFC) alterations, two brain regions involved in learning and memory processes (Bussière et al., 2003; West et al., 1994). Therefore, the present study investigated the effects of LIG on learning and memory deficits induced by bilateral intracerebroventricular (icv) injections of $A\beta_{25-35}$, the core of $A\beta_{1-42}$ neurotoxic fragment, in rats, as well as the neuropathological and inflammatory alterations in the PFC and CA1 subregion of the hippocampus.

## 2. Materials and methods

### 2.1. Animals

Male SPF Wistar rats (8 week old weighing 250–300 g) were used in the present study. The rats were obtained from the Institute of Experimental Animals, Sichuan Academy of Medical Sciences. The animals were acclimatized for 5 days at 22 ± 1 °C with a 12-h light–dark cycle and allowed free access to drinking water and a commercial pellet diet obtained from the institute. All animal experiments were performed in accordance with the Regulations of Experimental Animal Administration issued by the State Committee of Science and Technology of the People's Republic of China (November 14, 1988).

### 2.2. $A\beta_{25-35}$ intracerebroventricular injections and drug administration

$A\beta_{25-35}$ (Lot no. 115k4778, Sigma, St. Louis, MO) was incubated at 37 °C for 7 days to reduce the possibility of rapid coagulation and to allow diffusion of the peptide into the brain. Rats were anesthetized with intraperitoneal injection of 40 mg/kg sodium pentobarbital (Lot no. 020919, Sinopharm Chemical Reagent Co., Ltd., Shanghai, China) and placed on a stereotaxic apparatus with rectal temperature maintained at 37 °C using a heating pad. An area of skin on top of the skull was shaved and sterilized conventionally. Two small holes for needle insertion were drilled in the parietal bone posterior to bregma on either side of the midline (coordinates: anterior/posterior −0.8 mm, medial/lateral ±1.5 mm relative to bregma, dorsal/ventral −3.8 mm below dura; Paxinos and Watson, 1997). Animals were randomly assigned to three groups: sham, LIG, and vehicle ($n = 10$ per group). $A\beta_{25-35}$ (50 nmol in 10 μl of saline) was injected icv bilaterally in the LIG- and vehicle-treated groups via a stainless steel needle using a microinjector. $A\beta_{25-35}$ solution was injected into each of the lateral cerebral ventricles over a 5-min period with a 5-min waiting period between the two injections. The sham control group underwent all surgical steps, with the exception that saline was administered rather than $A\beta_{25-35}$. Following wound suturing, all rats received an intramuscular injection of 40,000 unit/0.25 ml of the antibiotic penicillin (Lot no. C05010716, Harbin Pharmaceutical Group Co., Ltd., General Pharmaceutical Factory, Harbin, China).

LIG was prepared by a well-established procedure in our laboratory. LIG purity (Lot no. 20070806) was determined to be >98% based on the percentage of total peak area assessed by high-performance liquid chromatography. LIG was prepared with 3% Tween-80 before use. LIG (40 mg/kg), the effective dose in vascular dementia (Kuang et al., 2008), or volume-matched vehicle was orally administered 1 h before icv injection of $A\beta_{25-35}$ and once daily for 15 days according to the assigned groups.

### 2.3. Morris water maze

Cognitive function was evaluated in the Morris water maze (Morris, 1984; Kuang et al., 2008). The maze consisted of a black circular pool (1.2 m diameter, 40 cm height) filled with water (22 ± 1 °C) to a depth of 20 cm. A circular platform (14 cm diameter) was submerged 2 cm below the surface of the water and hidden from the rat's view. At the beginning of each day, the water was made opaque by adding 2 kg of milk to prevent the animals from seeing the submerged platform. Four points, equally spaced along the circumference of the pool, were arbitrarily assigned as North, South, East, and West. The pool, therefore, was divided into four quadrants (Northeast, Southeast, Southwest, and Northwest). These points served as the starting positions for the rat being gently lowered into the water, with its head facing the wall of the tank. The water maze test consisted of four stages: Days 1–5 for hidden platform training before icv injection of $A\beta_{25-35}$, Days 14–16 for a "post-treatment" hidden platform latency test, Day 17 for a probe test, and Days 18–20 for a reversal trial. LIG or vehicle were administered once daily during Days 6–20. The behavioral tests were performed 1 h after LIG or vehicle treatment.

#### 2.3.1. Hidden platform trial

Rats were given two trials per day with a submerged platform that they could climb onto to escape from the water. The location of the platform was fixed in the middle of the NE quadrant, 30 cm from the wall, throughout training. Two starting points, equidistant from the platform, were used. The starting points were different for consecutive trials but were counterbalanced to prevent possible order effects. At the beginning of each trial, the rat was gently placed into the water at the start location, always facing the side of the tank. A trial ended when the rat escaped onto the platform, and the escape latency for each trial was recorded. If a rat failed to escape within 60 s, an escape latency of 60 s was recorded. Each rat was allowed to spend 10 s on the escape platform and then was placed for an additional 20 s in a holding cage before the next trial, resulting in an intertrial interval of 35 s. The mean escape latency of each daily trial was then calculated.

#### 2.3.2. Probe trial

In this 1-day test, each rat was subjected to a probe trial (60 s) in which no platform was present on which to escape. One of two starting positions in the hidden platform trial was used and was consistent for all rats. For the probe trial, two measurements were made: (1) time spent in the quadrant of the former platform position and (2) number of crossings of the exact location where the platform had been located previously.

#### 2.3.3. Reversal trial

Rats were given a reversal trial similar to the hidden platform trial, with the exception that the platform was located in a novel position opposite to the location used in the hidden platform trial.

### 2.4. Tissue processing

At the end of the behavioral testing on Day 20, rats were deeply anesthetized with 3.5% chloral hydrate (350 mg/kg, i.p.; Tianjin Kermel Chemical Reagent Development Center, Tianjin, China) and subsequently perfused transcardially with phosphate-buffered saline (PBS) followed by 4% paraformaldehyde fixative. The brains then were removed and embedded in paraffin.

### 2.5. Histopathological examination

To detect the neuronal integrity, the brains were cut into approximately 5 μm sections and stained with hematoxylin and eosin. In each PFC and CA1 subregion of the hippocampus, the number of intact-appearing neurons and pyramidal cells showing a distinct nucleus and nucleolus was counted along a 1.35 mm transection (×400 magnification). For quantitative analysis, we took five rats from each group. Thus, three slides were taken from each rat, and a total of 15 sections (five rats) from each group were counted. The number of the PFC neurons and pyramidal cells per $mm^2$ in each group was expressed as the mean of the 15 sections.

Immunohistochemistry analysis was used to examine the immunoreactivities of AD neuropathological markers and neuroinflammatory mediators according to the avidin–biotin complex (ABC) kit procedure (Wuhan Boster Biological Technology, Wuhan, China].

Briefly, the sections of PFC and CA1 subregion of the hippocampus were rinsed with 3% $H_2O_2$ for 15 min to block endogenous peroxide activity and incubated with 5% bovine serum albumin from the ABC kit for 30 min to block nonspecific binding. The sections then were incubated with respective rabbit polyclonal antibodies (Wuhan Boster Biological Technology, Wuhan, China) against Aβ (1:100), APP (1:50), p-Tau (1:100), TNF-α (1:100), and NF-κB (1:100) diluted in PBS overnight at 4 °C. Primary antibodies were recognized by biotinylated anti-rabbit secondary antibody at 37 °C for 1 h and detected by ABC at 37 °C for 1 h. Immunoreactions were visualized using 3,3′-diaminobenzidine tetrahydrochloride (DAB) as a chromagen. Negative controls were prepared identically except for the omission of primary antibodies. For quantitative analysis of immunohistochemical results, brain sections were observed under a light microscope by an investigator who was blind to section identification. Photomicrographs were taken using a Leica Digital Camera DC 300 (Leica Microsystems, Heerbrugg, Switzerland). Immunoreactivity was quantified on the basis of the integrated optic density of the positive immunostained cells using Image Pro Plus 5.02 software (Media Cybernetics, Bethesda, MD). Three slides were taken from each rat and processed immunohistochemically; thus, a total of 15 sections from five rats from each group were examined for each marker.

### 2.6. Statistic analysis

All experimentation was performed by observers blind to treatment and histological assessment. Data analyses were performed with SPSS 11.5. Data obtained over training days from the hidden platform trial and reversal trial were analyzed by two-way analysis of variance (ANOVA). Mean escape latency was the dependent variable, day was the within-subjects variable, and the three groups were the between-subjects variables. When appropriate, *post hoc* comparisons were made using the Least Significant Difference (LSD) test (equal variances assumed) or Dunnett's T3 test (equal variances not assumed). The remaining data were analyzed by one-way ANOVA. All results are expressed as mean ± SD. Values of $p<0.05$ were considered statistically significant.

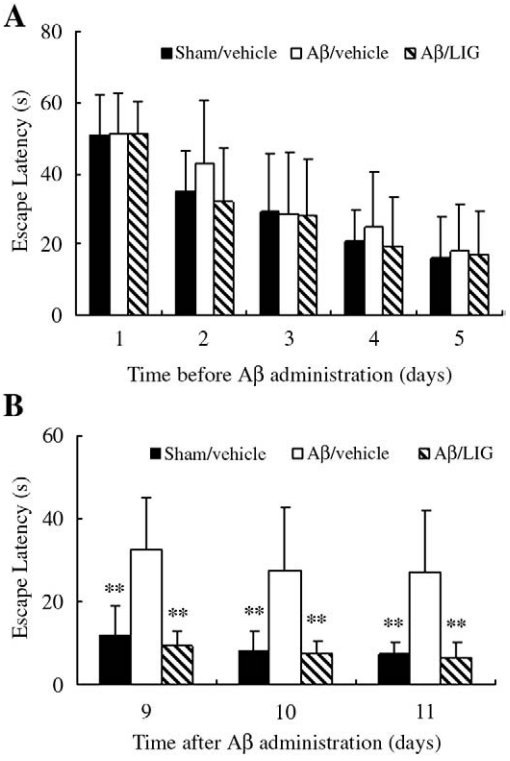


**Fig. 1.** Comparison of average escape latencies for each group in the hidden platform trial before and after LIG treatment in rats (A) before $A\beta_{25-35}$ administration and (B) 9 to 11 days after $A\beta_{25-35}$ administration. LIG (40 mg/kg) was orally administered 1 h before bilateral icv injections of 50 nmol $A\beta_{25-35}$ and once daily. Data points indicate the average latency to find the platform and are expressed as mean ± SD ($n=10$ each group). $^{**}p<0.01$ *vs.* vehicle-treated group.

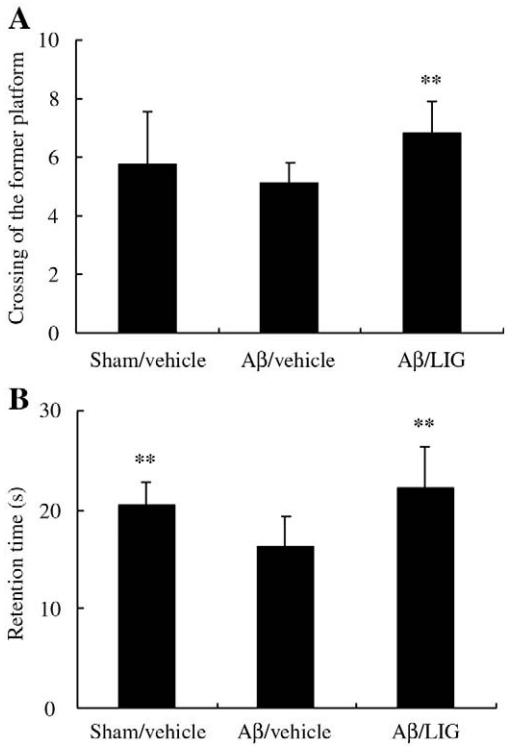


**Fig. 2.** Performance in the probe trial test for each group after LIG treatment in rats. (A) Crosses over the former platform location. (B) Time spent in the quadrant of the former platform position. Data are expressed as mean ± SD ($n=10$ each group). $^{**}p<0.01$ *vs.* vehicle-treated group.

## 3. Results

### 3.1. Effect of LIG on $A\beta_{25-35}$-induced impairments in cognition function

Before icv injection of $A\beta_{25-35}$, the escape latencies in the hidden platform trial for the sham-operated group, LIG-treated group, and vehicle group all decreased in a day-dependent manner. No significant differences were observed among groups (Fig. 1A). After 9 to 11 days of treatment following $A\beta_{25-35}$ administration, a significant difference was found in escape latency among groups ($F_{2,\ 27}=39.116$, $p<0.001$). The group treated with LIG (40 mg/kg, p.o.) showed a significant decrease in escape latency compared to the vehicle-treated group ($p<0.01$). No statistically significant difference was observed between the LIG-treated and sham-operated groups ($p>0.05$, Fig. 1B).

Finding a hidden platform can be accomplished with some proficiency without animals employing a “spatial” strategy. Thus, the probe trial was employed to determine how well the rats located the platform in the maze. On Day 12 after $A\beta_{25-35}$ administration, data were obtained from two measures of probe trial performance (Fig. 2A and B). The group that received LIG treatment (40 mg/kg, p.o.) spent more time than the vehicle-treated group in the training quadrant where the platform was previously located ($p<0.01$). The vehicle group visited all quadrants equally during 60 s of free swimming (Fig. 2A). Similar results were obtained from crossings of the former platform location in the probe trial. The rats treated with LIG (40 mg/kg, p.o.) crossed over the platform location more frequently than vehicle-treated rats ($p<0.01$, Fig. 2B).

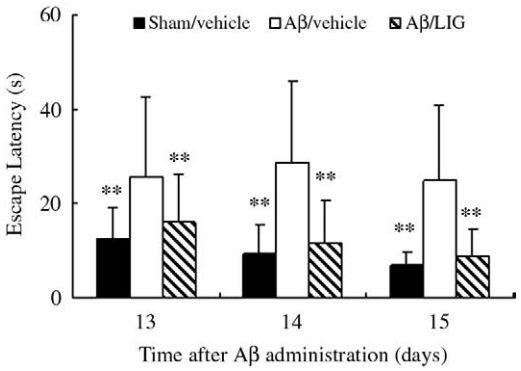


**Fig. 3.** Performance in the reversal trial (new platform test) for each group after LIG treatment in rats. Data points represent the average latency to find the platform ($n=10$ each group). $^{**}p<0.01$ *vs.* vehicle-treated group.

The average latency in the reversal trial was the time spent by rats finding the platform located in a different quadrant (SW) than the one (NE) used in the hidden platform trial. After 13 to 15 days of treatment following $A\beta_{25-35}$ administration, a significant difference in the successive three training days was observed among groups ($F_{2,27}=17.446$, $p<0.001$, Fig. 3). The group treated with LIG (40 mg/kg, p.o.) spent significantly less time finding the platform than the vehicle-treated group ($p<0.01$).

### *3.2. Effects of LIG on $A\beta_{25-35}$-induced AD neuropathological marker immunoreactivity*

Typical neuropathological changes occurred in the rat PFC and CA1 subregion of the hippocampus 15 days after icv injections of $A\beta_{25-35}$. Neuronal loss, shrinkage, and dark staining of neurons were observed in the PFC and hippocampal CA1 in vehicle-treated rats (Fig. 4A). LIG (40 mg/kg, p.o.) greatly attenuated these $A\beta_{25-35}$-induced pathomorphologic changes. The neuroprotective effect of LIG was determined by quantitative analysis of the number of neurons in both the PFC and hippocampal CA1 subregion (Fig. 4B and C). LIG significantly inhibited $A\beta_{25-35}$-induced neuronal loss compared with vehicle-treated animals ($p<0.01$).

The effects of LIG on Aβ, APP, and p-Tau immunoreactivity in the PFC and hippocampal CA1 subregion are shown in Fig. 5A and B. $A\beta_{25-35}$ increased the expression of Aβ, APP, and p-Tau in the rat PFC and hippocampal CA1 subregion in the vehicle group, effects that were significantly prevented by LIG treatment (40 mg/kg, p.o.) for 15 days ($p<0.01$, Fig. 5C). The immunostaining of Aβ, APP, or p-Tau was not significantly detected in sham control rats.

### *3.3. Effects of LIG on $A\beta_{25-35}$-induced neuroinflammatory mediator immunoreactivity*

TNFα and NF-κB immunostaining is shown in Fig. 6A. $A\beta_{25-35}$ increased the expression of TNFα and NF-κB in the rat hippocampal and hippocampal CA1 subregion of the vehicle group, and LIG (40 mg/kg, p.o.) treatment significantly prevented the $A\beta_{25-35}$-induced increase of NF-κB immunoreactivity compared to vehicle-treated rats ($p<0.01$, Fig. 6B). TNFα or NF-κB immunostaining was not significantly detected in the sham control group.

## 4. Discussion

Learning and memory deficits are the early clinical manifestations of AD. In the present study, the Morris water maze test was used to examine cognitive function (Morris 1984; Moser et al., 1995). In general, cognition includes at least three primary processes: acquisition, consolidation, and retention. In the Morris water maze test, the hidden platform trial

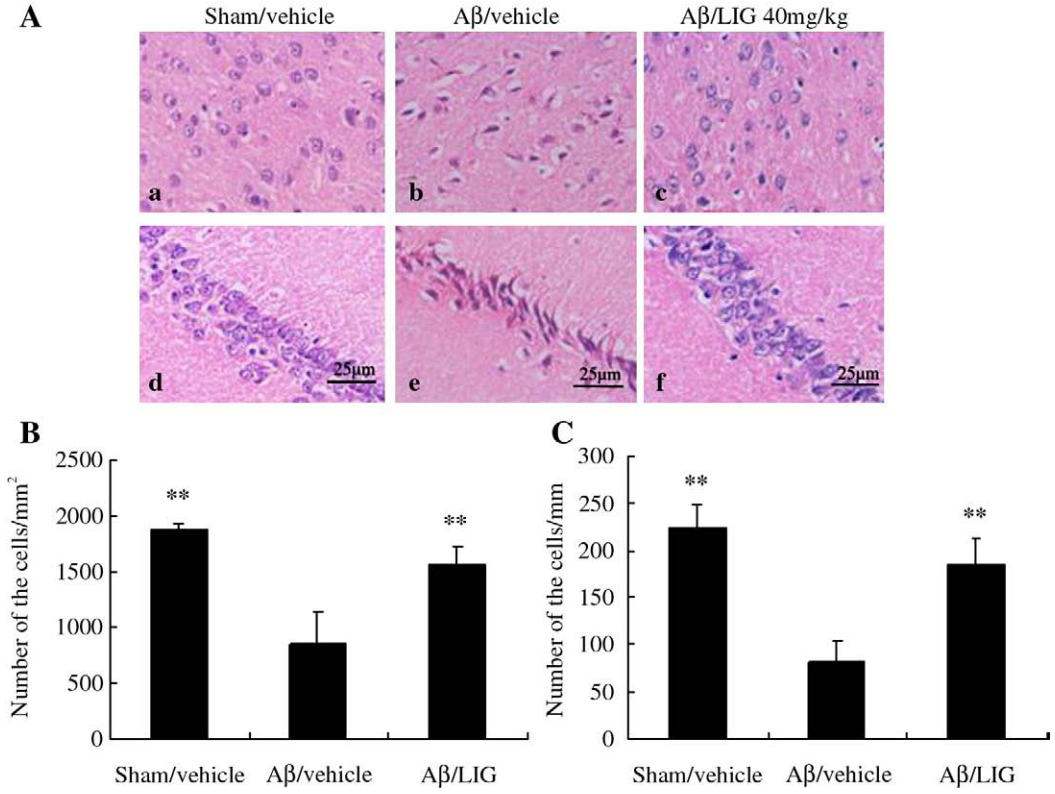


**Fig. 4.** Effects of LIG on the neuropathological changes induced by $A\beta_{25-35}$ in the prefrontal cortex and hippocampal CA1 subregion in rats. LIG (40 mg/kg) was orally administered 1 h before bilateral icv injections of 50 nmol $A\beta_{25-35}$ and once daily for 15 days. Intact-appearing neurons were counted in a high power field (×400 magnification). (A) Photomicrographs of histopathological changes in the rat prefrontal cortex (a, b, c) and hippocampal CA1 subregion (d, e, f). (B) Quantitative analysis of the neurons in the rat prefrontal cortex. (C) Quantitative analysis of the neurons in the rat hippocampal CA1 subregion. Values are expressed as mean ± SD ($n=5$ each group). $^{**}p<0.01$ *vs.* vehicle-treated group.

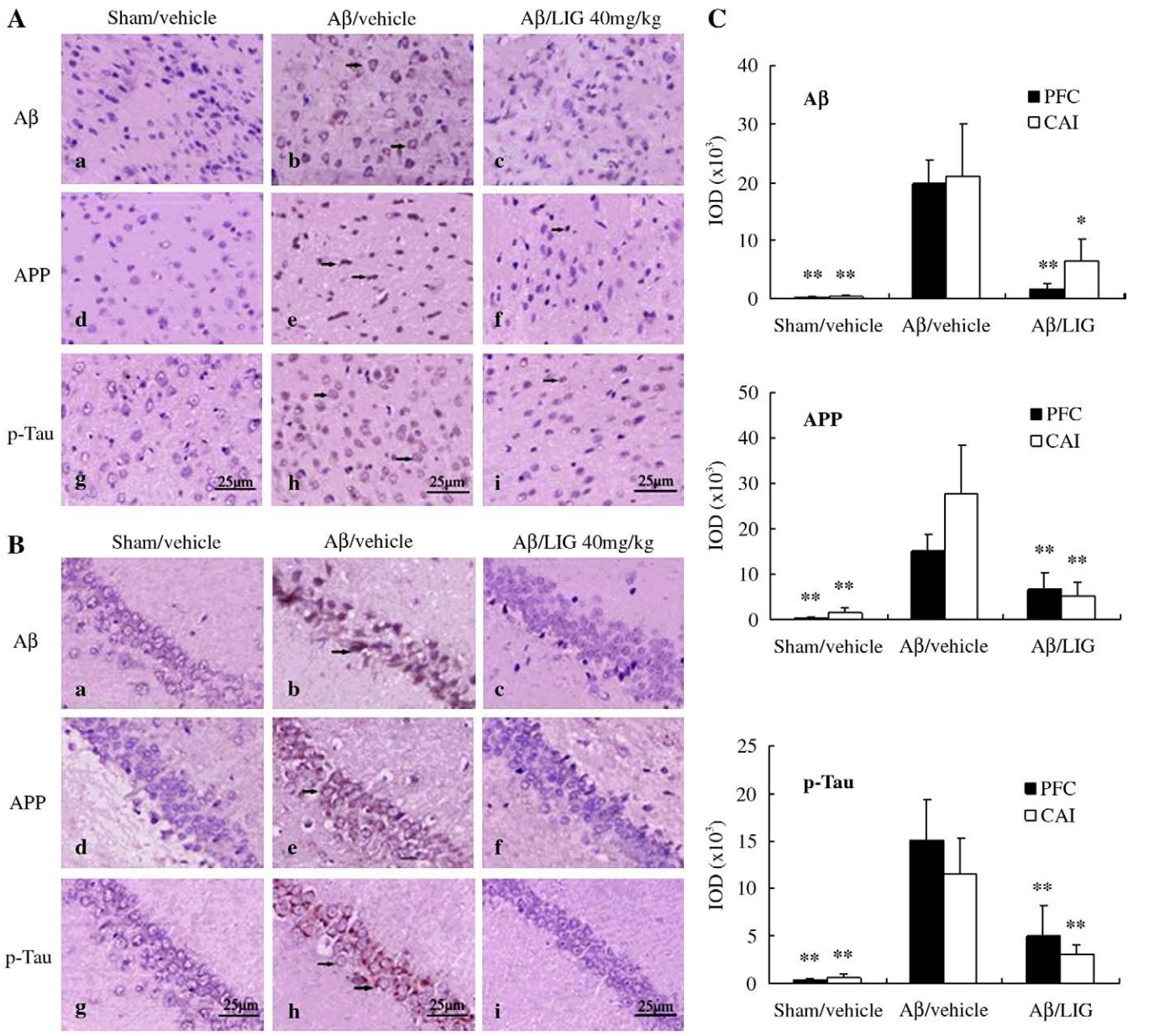


**Fig. 5.** Effects of LIG on Aβ, APP, and p-Tau expression induced by $A\beta_{25-35}$ in rats. LIG (40 mg/kg) was orally administered 1 h before bilateral icv injections of 50 nmol $A\beta_{25-35}$ and once daily for 15 days. The black arrowheads indicate immunopositive cells. (A) Photomicrographs of immunohistochemical changes in the rat prefrontal cortex (PFC). (B) Photomicrographs of immunohistochemical changes in the rat hippocampal CA1 subregion (CA1). (C) Quantification of the immunohistochemical analysis in the PFC and CA1 in rats by determining the integrated optic density (IOD) of the positive immunostained cells using Image Pro Plus 5.02 software. Values are expressed as mean ± SD ($n = 5$ each group). $^{*}p<0.05$, $^{**}p<0.01$ *vs.* vehicle-treated group.

measured acquisition, the probe trial measured retention, and the reversal trial measured relearning ability (Kucukatay et al., 2002). Consistent with previous reports, the present study demonstrated that bilateral icv injections of 50 nmol $A\beta_{25-35}$, a core neurotoxic fragment of Aβ, induced significant impairment in learning and memory ability in rats (Whitehead et al., 2005). Nine to 15 days after $A\beta_{25-35}$ administration, the rats in the vehicle-treated group tended to circle the pool in the Morris water maze. Oral administration of 40 mg/kg LIG significantly decreased the latency of $A\beta_{25-35}$-treated rats to reach the platform in both the hidden platform trial and reversal trial compared with the vehicle controls. LIG treatment also increased the time that $A\beta_{25-35}$-administered rats spent swimming in the former quadrant and across the former position of the platform in the probe trial. These behavioral observations suggest that 40 mg/kg LIG could significantly prevent the cognitive dysfunction induced by icv injection of $A\beta_{25-35}$.

The neuronal alteration in hippocampus and cerebral cortex (e.g. prefrontal cortex and entorhinal cortex) plays an important role in AD-like cognitive deficits (Bussière et al., 2003; Gomez-Isla et al., 1996; West et al., 1994). The complex behaviors, such as those evaluated in the water maze test, depend on the coordinated function of several brain structures. For practical reasons as described previously (Trabace et al., 2007), we detected in the present study the neuronal changes in the PFC and hippocampal CA1 subregion of rats after icv injection of Aβ through HE staining. The findings indicated that 40 mg/kg LIG could significantly preserved the number of neurons in both the PFC and CA1 subregion of $A\beta_{25-35}$-treated rats. Moreover, neuropathological changes in AD patients are well accepted to be mainly characterized by neurofibrillary tangles, senile plaques, and neuronal loss. Studies indicate that neurofibrillary tangles originate from abnormal phosphorylation of the Tau protein that normally exists as a cytoskeleton protein in neurons

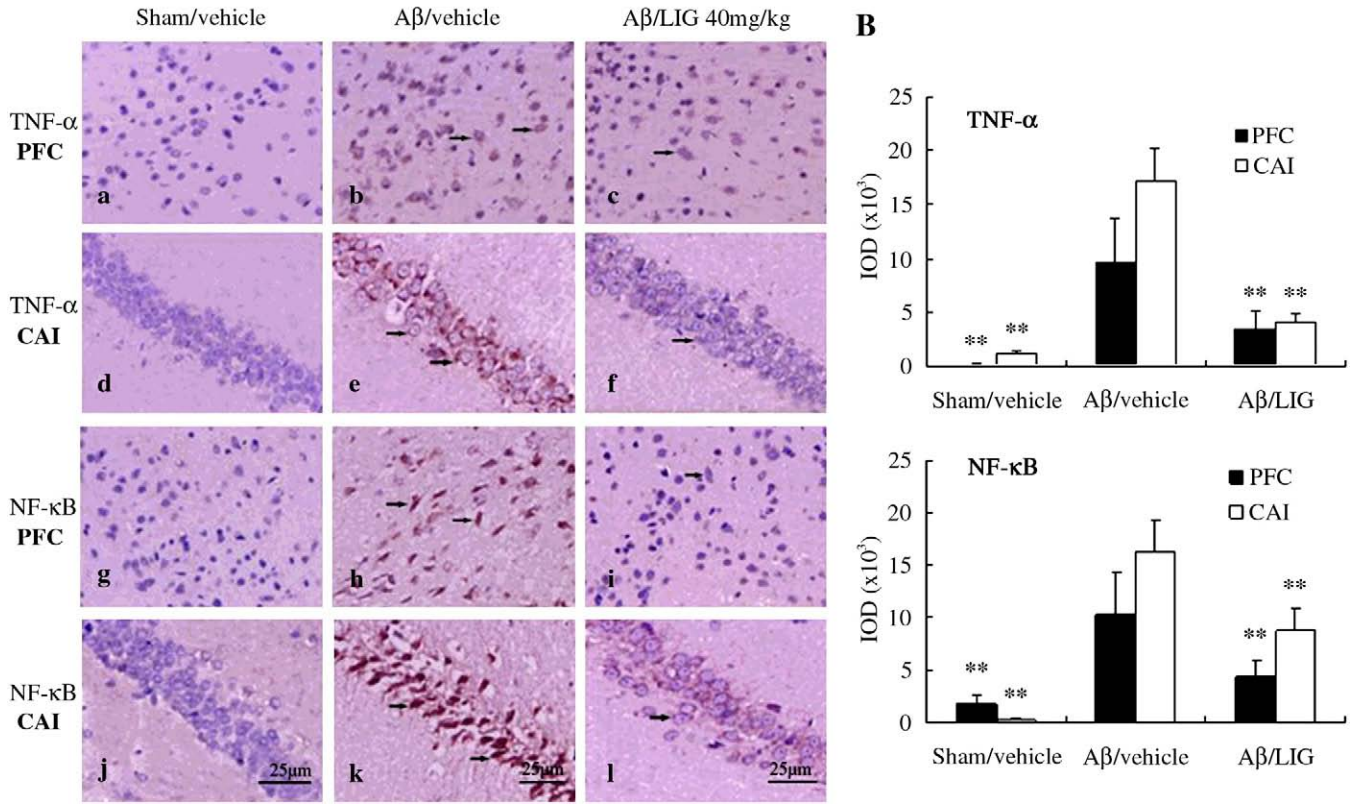


**Fig. 6.** Effects of LIG on TNFα and NF-κB expression induced by $A\beta_{25-35}$ in rats. LIG (40 mg/kg) was orally administered 1 h before bilateral icv injections of 50 nmol $A\beta_{25-35}$ and once daily for 15 days. The black arrowheads indicate immunopositive cells. (A) Photomicrographs of immunohistochemical changes in the rat prefrontal cortex (PFC) and hippocampal CA1 subregion (CA1). (B) Quantification of the immunohistochemical analysis in the PFC and CA1 subregion by determining the integrated optic density (IOD) of positive immunostained cells using Image Pro Plus 5.02 software. Values are expressed as mean ± SD ($n = 5$). $^{**}p<0.01$ *vs.* vehicle-treated group.

(Kosik et al., 1986). Senile plaques mainly comprise $A\beta_{1-40}/A\beta_{1-42}$ formed by the photolytic cleavage of APP (Selkoe et al., 1986) that can be upregulated by icv administration of $A\beta_{25-35}$ (Cheng et al., 2006). Abnormal phosphorylation of Tau and the expression of APP or Aβ have been proposed to be necessary for the formation of neurofibrillary tangles and senile plaques following Aβ toxic insult, respectively, in an $A\beta_{25-35}$-mediated early Alzheimer's disease model in rats. In the present study, the p-Tau antibody pSer202, specific for an "activated" Tau protein (p-Tau), was used to detect the expression of p-Tau. Additionally, we examined endogenous Aβ immunoreactivity with an anti-$A\beta_{1-40}$ antibody not recognizing exogenously injected $A\beta_{25-35}$ fragments. The immunohistochemical results showed that bilateral icv injections of $A\beta_{25-35}$ significantly increased Aβ, APP, and p-Tau immunoreactivity in both the rat PFC and hippocampal CA1 subregion, an effect that was effectively prevented by oral administration of 40 mg/kg LIG. The amyloidogenic fragment of APP, endogenous Aβ, is generated by β- and γ-secretases, whereas cleavage of APP by α-secretase produces the non-amyloidogenic fragment sAPPα. Although the present study did not explore the potential mechanisms involved in the inhibitory effects of LIG on Tau phosphorylation and endogenous Aβ formation, our results suggest that LIG may prevent AD-like formation of neurofibrillary tangles and senile plaques by inhibiting hyperphosphorylation of the Tau protein and endogenous Aβ production in rats receiving $A\beta_{25-35}$. Furthermore, consistent with previous studies (Klementiev et al., 2007), the present histopathological results showed that icv administration of $A\beta_{25-35}$ induced numerous degenerating neurons with chromatolysis and eccentrically dispersed nuclei in the PFC and hippocampal CA1 subregion, whereas treatment with 40 mg/kg LIG prevented neuronal damage and preserved neurons.

The accumulation of Aβ plaques in the AD brain results in glial cell activation and initiates neuroinflammatory responses, a process in which the NF-κB-dependent pathway plays an important role (Akama et al., 1998; Akiyama et al., 2000; Hu and Van Eldik, 1999). As a multifunctional pro-inflammatory cytokine, TNF-α is a potent stimulator of NF-κB, a transcription factor that elevates the expression of pro-inflammatory factors such as cyclooxygenase (Bales et al., 1998). In the present study, NF-κB activation was detected with antibody staining of NF-κB p65 subunits. Our results showed that 40 mg/kg LIG significantly reduced TNFα and activated NF-κB immunostaining in the brains of rats receiving injections of $A\beta_{25-35}$ injection. This study demonstrated that the anti-inflammatory effect of LIG may be the mechanism by which it provides protection against $A\beta_{25-35}$ neurotoxicity in rats.

Despite the extensive study with Aβ peptide, the mechanism of Aβ-induced neurotoxicity and cognitive impairments remains unclear. The converging evidence suggest that intracellular calcium accumulation, reactive oxygen species and nitric oxide productions, decreased membrane fluidity, alteration of the cytoskeleton and nucleus, and inflammatory or autoimmune process are probably involved in the mechanisms of Aβ-induced neurotoxicity (Huang and Jiang, 2009; Walsh et al., 2002). Therefore, a number of new neuroprotective agents targeted on these potential AD pathogenesis, are under investigation. For example, the studies on the therapeutic effects of anti-inflammatory agents or antioxidants for the treatment of AD have produced promising results (Hirohata et al., 2008; Ono et al., 2006). This is the first study examining the role of LIG as an anti-inflammatory agent in an experimental model of AD in young rats (8 week old). In addition, our previous studies have demonstrated that LIG at a dose of 40 mg/kg significantly protected against cerebral ischemic damage via multiple of pharmacological activities including antioxidant and antiapoptotic effects as well as cholinergic activity enhancement (Kuang et al., 2006; Kuang et al., 2008; Yu et al., 2008).

Therefore, LIG would be a potential candidate for further preclinical study aimed at the prevention and treatment of cognitive deficits in AD. The detailed dose–effect relationship and overall mechanisms of LIG are under investigation in aged AD animals.

Taken together, the present results from both the behavioral testing and histochemical analysis demonstrated that the protection of LIG against Aβ neurotoxicity could be associated with the improvements seen in cognitive deficits and neuropathological alterations in the rat. Moreover, the inhibitory effect on TNF-α-activated NF-κB signaling pathway may contribute to the neuroprotective potential of LIG in Aβ neurotoxicity.

## References


Akama KT, Albanese C, Pestell RG, Van Eldik LJ. Amyloid β-peptide stimulates nitric oxide production in astrocytes through an NFκB-dependent mechanism. Proc Natl Acad Sci U S A 1998;95:5795–800.

Akiyama H, Barger S, Barnum S, Bradt B, Bauer J, Cole GM, et al. Inflammation and Alzheimer's disease. Neurobiol Aging 2000;21:383–421.

Bales KR, Du Y, Dodel RC, Yan GM, Hamilton-Byrd E, Paul SM. The NF-κB/Rel family of proteins mediates Aβ-induced neurotoxicity and glial activation. Mol Brain Res 1998;57:63–72.

Bales KR, Du Y, Holtzman D, Cordell B, Paul SM. Neuroinflammation and Alzheimer's disease: critical roles for cytokine/Aβ-induced glial activation, NF-κB, and apolipoprotein E. Neurobiol Aging 2000;21:427–32.

Bussière T, Giannakopoulos P, Bouras C, Perl DP, Morrison JH, Hof PR. Progressive degeneration of nonphosphorylated neurofilament protein-enriched pyramidal neurons predicts cognitive impairment in Alzheimer's disease: stereologic analysis of prefrontal cortex area 9. J Comp Neurol 2003;463:281–302.

Cheng G, Whitehead SN, Hachinski V, Cechetto DF. Effects of pyrrolidine dithiocarbamate on Aβ (25–35)-induced inflammatory responses and memory deficits in the rat. Neurobiol Dis 2006;23:140–51.

Colton CA, Chernyshev ON, Gilbert DL, Vitek MP. Microglial contribution to oxidative stress in Alzheimer's disease. Ann N Y Acad Sci 2000;899:292–307.

Eikelenboom P, Veerhuis R, Familian A, Hoozemans JJ, van Gool WA, Rozemuller AJ. Neuroinflammation in plaque and vascular β-amyloid disorders: clinical and therapeutic implications. Neurodegener Dis 2008;5:190–3.

Gomez-Isla T, Price JL, McKeel Jr DW, Morris JC, Growdon JH, Hyman BT. Profound loss of layer II entorhinal cortex neurons occurs in very mild Alzheimer's disease. J Neurosci 1996;16:4491–500.

Hirohata M, Ono K, Yamada M. Non-steroidal anti-inflammatory drugs as anti-amyloidogenic compounds. Curr Pharm Des 2008;14:3280–94.

Hu J, Van Eldik LJ. Glial-derived proteins activate cultured astrocytes and enhance beta amyloid-induced glial activation. Brain Res 1999;842:46–54.

Huang HC, Jiang ZF. Accumulated amyloid-beta peptide and hyperphosphorylated Tau protein: relationship and links in Alzheimer's disease. J Alzheimers Dis 2009;16:15–27.

Husain MM, Trevino K, Siddique H, McClintock SM. Present and prospective clinical therapeutic regimens for Alzheimer's disease. Neuropsychiatric Dis Treat 2008;4:765–77.

Klementiev B, Novikova T, Novitskaya V, Walmod PS, Dmytriyeva O, Pakkenberg B, et al. A neural cell adhesion molecule-derived peptide reduces neuropathological signs and cognitive impairment induced by $A\beta_{25-35}$. Neurosci 2007;145:209–24.

Kosik KS, Joachim CL, Selkoe DJ. Microtubule-associated protein tau (τ) is a major antigenic component of paired helical filaments in Alzheimer disease. Proc Natl Acad Sci U S A 1986;83:4044–8.

Kuang X, Yao Y, Du JR, Liu YX, Wang CY, Qian ZM. Neuroprotective role of Z-ligustilide against forebrain ischemic injury in ICR mice. Brain Res 2006;1102:145–53.

Kuang X, Du JR, Liu YX, Zhang GY, Peng HY. Postischemic administration of Z-ligustilide ameliorates cognitive dysfunction and brain damage induced by permanent forebrain ischemia in rats. Pharmacol Biochem Behav 2008;88:213–21.

Kucukatay V, Balkan S, Yaras N, Yargicoglu P, Agar A. The effect of pergolide on cognitive performance of young and middle-aged rats. Int J Neurosci 2002;112:1027–36.

Lin M, Zhu GD, Sun QM, Fang QC. Chemical studies of Angelica sinensis. Acta Pharmceut Sin 1979;14:529–34.

Liu L, Ning ZQ, Shan S, Zhang K, Deng T, Lu XP, et al. Phthalide lactones from *Ligusticum chuanxiong* inhibit lipopolysaccharide-induced TNF-α production and TNF-α-mediated NF-κB activation. Planta Med 2005;71:808–13.

McGeer PL, McGeer EG. Inflammation, autotoxicity and Alzheimer disease. Neurobiol Aging 2001;22:799–809.

Morris R. Developments of a water maze procedure for studying spatial learning in the rat. J Neurosci Methods 1984;11:47–60.

Moser MB, Moser EI, Forrest E, Andersen P, Morris RG. Spatial learning with a minislab in the dorsal hippocampus. Proc Natl Acad Sci U S A 1995;92:9697–701.

Naito T, Ikeya Y, Okada M, Mistuhashi H, Maruno M. Two phthalides from Ligusticum chuanxiong. Phytochemistry 1996;41:233–6.

Ono K, Hamaguchi T, Naiki H, Yamada M. Anti-amyloidogenic effects of antioxidants: implications for the prevention and therapeutics of Alzheimer's disease. Biochem Biophys Acta 2006;1762:575–86.

Pasinetti GM. From epidemiology to therapeutic trials with anti-inflammatory drugs in Alzheimer's disease: the role of NSAIDs and cyclooxygenase in β-amyloidosis and clinical dementia. Alzheimers Dis 2002;4:435–45.

Paxinos G, Watson C. The Rat Brain in Stereotaxic Coordinates. 2nd edn. San Diego: Academic Press; 1997.

Peng HY, Du JR, Zhang GY, Kuang X, Liu YX, Qian ZM, et al. Neuroprotective effect of Z-ligustilide against permanent focal ischemic damage in rats. Biol Pharm Bull 2007;30:309–12.

Selkoe DJ, Abraham CR, Podlisny MB, Duffy LK. Isolation of low-molecular-weight proteins from amyloid plaque fibers in Alzheimer's disease. J Neurochem 1986;46:1820–34.

Trabace L, Kendrick KM, Castrignanò S, Colaianna M, De Giorgi A, Schiavone S, et al. Soluble amyloid beta $_{1-42}$ reduced dopamine levels in rat prefrontal cortex: relationship to nitric oxide. Neurosci 2007;147:652–63.

Walsh DM, Klyubin I, Fadeeva JV, Roman MJ, Selkoe DJ. Amyloid-beta oligomers: their production, toxicity and therapeutic inhibition. Biochem Soc Trans 2002;30:552–7.

West MJ, Coleman PD, Flood DG, Troncoso JC. Differences in the pattern of hippocampal neuronal loss in normal ageing and Alzheimer's disease. Lancet 1994;344:769–72.

Whitehead SN, Hachinski VC, Cechetto DF. Interaction between a rat model of cerebral ischemia and beta-amyloid toxicity: inflammatory responses. Stroke 2005;36:107–12.

Yu Y, Du JR, Wang CY, Qian ZM. Protection against hydrogen peroxide-induced injury by Z-ligustilide in PC12 cells. Exp Brain Res 2008;184:307–12.